Annals of Biomedical Engineering, Vol. 35, No. 5, May 2007 (© 2007) pp. 847–857
DOI: 10.1007/s10439-007-9253-6

Nonlinear Dynamic Model of CA1 Short-Term Plasticity using Random Impulse Train Stimulation

GHASSAN GHOLMIEH,[1] SPIROS COURELLIS,[2] VASILIS MARMARELIS,[2] and THEODORE BERGER[2,3]

[1]Division of Neurology, Childrens Hospital Los Angeles, 4650 Sunset Blvd, MS 82, Los Angeles, CA, 90027, USA; [2]Department of Biomedical Engineering, USC, Los Angeles, CA, 90089-1451, USA; and [3]Neuroscience Program, USC, Los Angeles, CA, 90089-2520, USA

(*Received 9 July 2006; accepted 3 January 2007; published online 23 March 2007*)

Abstract—A comprehensive, quantitative description of the nonlinear dynamic characteristics of the short-term plasticity (STP) in the CA1 hippocampal region is presented. It is based on the Volterra–Poisson modeling approach using random impulse train (RIT) stimuli. *In vitro* hippocampal slice preparations were used from adult rats. RIT stimuli were applied at the Schaffer collaterals and population spike responses were recorded at the CA1 cell body layer. The computed STP descriptors that capture the nonlinear dynamics of the underlying STP mechanisms were the Volterra–Poisson kernels. The kernels quantified the presence of facilitatory and inhibitory STP behavior in magnitude and duration. A third order Volterra–Poisson STP model was introduced that accurately predicted in-sample and out-of-sample system responses. The proposed model could also accurately predict impulse pair and short impulse train system responses.

Keywords—CA1, Multielectrode array, Nonlinear analysis, Paired pulse, Random impulse train, Short-term plasticity, Kernels.

INTRODUCTION

Short-Term Plasticity (STP) is a phenomenon where use dependent synaptic changes occur as a result of intense activity over a scale of seconds and wane back to the baseline.[36] Recently, there has been a growing interest in the information processing characteristics of STP, as it is thought to play an important role in habituation[6], learning[20] and temporal information processing.[1,5,12,14,18]

The weight of evidence for neural encoding points to the temporal relationship of the cell output (firing frequency, EPSP, Population Spike) to its presynaptic input (synaptic current evoked by the impingement of electrical impulses [action potentials] on the nerve terminal).[27,11,24,28,29] This relationship has been traditionally investigated using paired impulse stimulation of variable interimpulse intervals[8,19,26] and short impulse trains at fixed frequencies.[5,4,7,25] The paired impulse approach is based on two-impulse stimuli separated in time by a variable time interval while the short impulse train approach uses impulse sequences at fixed interimpulse intervals. Fixed frequency impulse trains are thought to be more realistic stimuli since paired action potentials and paired population spikes rarely occur *in vivo*. Both methods provide *ad-hoc* quantitative descriptors of STP. They are, however, limited by the required long experimental time and by the type and the complexity of impulse interaction they can address.

Recently, several computational neuroscientists and electrophysiologists have utilized Poisson distributed Random Impulse Trains[2,3,30,32,34] and natural stimuli patterns[10] to study neuronal dynamics. The choice of Poisson distributed Random Impulse Trains (RIT) and natural stimuli patterns can be viewed as a hybrid between the paired impulse stimulation (variable interimpulse intervals) and the fixed frequency impulse train stimulation (the presence of an impulse sequence instead of only two impulses). However, the variety of analytical tools employed for data analysis in studies with this type of stimuli has not facilitated convergence in the conclusions and did not provide any type of relationship with paired impulse or short impulse train STP descriptors.

In this paper, we present quantitative descriptors of the nonlinear dynamics underlying the STP mechanisms in the CA1 hippocampal region. We applied the RIT stimuli to the Schaffer collaterals of CA1 *in vitro* preparations and recorded the corresponding population spike responses. We used the reduced Volterra–Poisson modeling approach[9,15,16] to compute the STP descriptors in the form of the reduced Volterra–Poisson kernels. We employed a third order model to capture and represent the nonlinear dynamic behavior of the underlying STP mechanisms. The computed

Address correspondence to Ghassan Gholmieh, Division of Neurology, Childrens Hospital Los Angeles, 4650 Sunset Blvd, MS 82, Los Angeles, CA, 90027, USA. Electronic mail: ggholmieh@chla.usc.edu

0090-6964/07/0500-0847/0 © 2007 Biomedical Engineering Society

quantitative STP descriptors (kernels) presented a comprehensive view of the excitatory and inhibitory STP behavior under a more realistic stimulation scenario. The resulting representation of STP provided a compact mathematical model with predictive capabilities, reducing the experimental time required for generating the new STP model considerably (compared to the impulse pair and short impulse train methods).

The article is organized into the following sections: (1) Materials and Methods, that describes the experimental setup, the data collection process, and the data analysis method; (2) Results, that presents estimates of the quantitative kernel STP descriptors of the CA1 hippocampal region *in vitro* and illustrates the predictive capabilities of the STP model; provides estimates of the STP mechanism's memory and presents STP facilitatory and inhibitory characteristics; compares the kernel STP descriptors with the Paired Impulse Facilitation Function (PIFF) describing STP when Paired Impulse stimulation is used and the Impulse Train Function (ITF) that describes STP when Impulse Train Stimuli are used; (3) Discussion, that concludes the article summarizing STP characteristics in the CA1 hippocampal region revealed by the kernel STP descriptors and by comparing the RIT approach with the impulse pair and the short impulse train approach.

MATERIALS AND METHODS

Biological Preparations & Hardware

Adult rats were decapitated after being fully anesthetized with Halothane. The hippocampus was extracted in a chilled aCSF bath and transverse slices (500 μm thick) were obtained using a Leika vibrotome (VT 100S). Each slice was positioned over a multielectrode array (Fig. 1) with the guidance of an inverted microscope (Leica DML 4×). A bipolar stimulation electrode (twisted Nichrome wires) was placed in the Schaffer collaterals region. The temperature was maintained at 30°C. Extracellular recordings were achieved using a microelectrode array. The setup consisted of a multimicroelectrode array (MEA-4[17]), pre-amplifiers, two data acquisition boards (Microstar, DAP 3200/214e series) at 7.35 kHz sampling rate per channel, and custom-developed software. The dataset from the channel with the strongest response (mean across channels: 421 μV, SD: 193 μV) was chosen for analysis. A Matlab based custom user interface was employed to control the data acquisition boards, perform data extraction, and conduct the data analysis.

Data Collection Process

In the beginning of each experiment, an Input–Output (I/O) curve was collected, forming a map

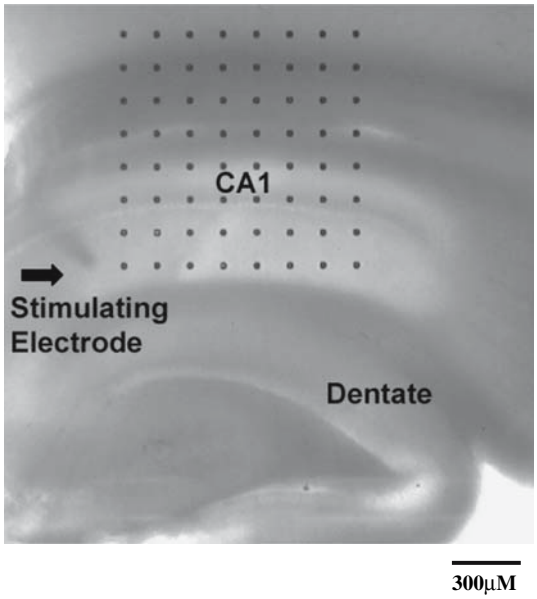

FIGURE 1. Picture of the hippocampal slice positioned over the multielectrode 8 × 8 array where each black dot represents an electrode.

between stimulus intensity and amplitude of the population spike response.[23,31,33] The stimulation intensity was adjusted to evoke a response with amplitude below 15% of the maximum population spike amplitude recorded in the I/O curve. Five stimulation sequences were then applied. Each stimulation sequence formed a subset of data and consisted of a pair of impulses 30 ms apart, followed by a random impulse train (RIT) of 200 pulses (Poisson Distributed with a mean rate of 2 Hz) 30 s later and 5 min of resting time. The interval between the beginning and the end of each stimulation sequence (paired pulse + RIT + 5 min of resting time) was approximately 7 min.

Data Analysis Methods

The data were preprocessed for electrophysiological stability and extraction of the amplitude of the population spike responses.[15] Each population spike response amplitude was assumed to be contemporaneous with its corresponding impulse stimulus.

Third order reduced Volterra–Poisson model

The data were analyzed using a variant of the Volterra–Poisson modeling approach, adapted for random impulse sequence stimuli and spike sequence responses.[9] The calculated first, second, and third order kernels served as the STP descriptors that captured STP nonlinear dynamics. They were also used to form a mathematical model of STP with predictive capabilities, expressed by the following equation:

$$y(n_i) = k_1 + \sum_{n_i-\mu<n_j<n_i} k_2(n_i - n_j) + \sum_{\substack{n_i-\mu<n_j<n_i \\ n_i-\mu<n_k<n_i}} k_3(n_i - n_j, n_i - n_k), \quad (1)$$

where n_i is the time of occurrence of the i-th impulse stimulus, n_j is the time of occurrence of the j-th impulse stimulus prior to the i-th impulse stimulus, n_k is the time of occurrence of the k-th impulse stimulus prior to the i-th impulse stimulus, $y(n_i)$ is the amplitude of the population spike response to the i-th impulse stimulus, μ is the memory of the biological system, k_1 is the first order kernel, k_2 is the second order kernel, and k_3 is the third order kernel. Equation 1 describes the amplitude of the population spike at time n_i in terms of the first order kernel k_1, the second order kernel k_2 (the effect of past impulse stimuli relative to the present impulse stimulus), and third order kernel k_3 (the effect of any past pair of impulse stimuli relative to the present impulse stimulus). The first order kernel represents the mean population spike amplitude. The first order kernel can also be thought of as the response to a single stimulus after a delay greater than or equal to the memory of the system. The second order kernel quantifies the effect on the current population spike amplitude of the interaction between the current impulse stimulus and each past impulse stimulus within the memory window μ. The third order kernel quantifies the effect on the current population spike amplitude of interaction between the present impulse and any two past impulses within the memory window μ (Fig. 2). In this article, the second and third order kernels were normalized with respect to the first order kernel.

For computational efficiency purposes, the Laguerre expansion method[21] was used to estimate the kernels. The second and third order kernels were expanded in the orthogonal associated Laguerre basis functions $L_l(m)$:

$$k_2(n_i - n_j) = \sum_{l=0}^{L-1} \gamma_l \mathscr{L}_l(n_i - n_j) \quad (2)$$

$$k_3(n_i - n_{j_1}, n_i - n_{j_2}) = \sum_{l_1} \sum_{l_2} \beta_{l_1,l_2} L_{l_1}(n_i - n_{j_1}) L_{l_2}(n_i - n_{j_2}),$$

where $\{\gamma_l\}$ and $\{\beta_{l_1,l_2}\}$ are the Laguerre coefficients and

$$L_l(m) = \alpha^{\frac{m-1}{2}}(1-\alpha)^{\frac{1}{2}} \sum_{k=0}^{l} (-1)^k \binom{n}{k} \binom{1}{k} \alpha^{(l-k)}(1-\alpha)^k \quad (3)$$

is the l-th order Laguerre function with $0 < \alpha < 1$. Substitution of the kernels in Eq. (1) with their expansion from Eqs. (2) results in an expression we use, in conjunction with the experimental data, to estimate the Laguerre coefficients via least square optimization. The computed Laguerre coefficients are used in Eqs. (2) to estimate the kernels. The use of Laguerre basis functions provides smooth kernels estimates while it makes the kernel computation task considerably more tractable. It reduces the kernel estimation variance but increases the kernel estimation bias. A detailed discussion on the variability of the kernels computed via the Laguerre expansion method can be found in Westwick *et al.*[35]

The accuracy of the estimated kernels is assessed by the Normalized Mean Square Error (NMSE), defined as follows:

$$\mathrm{NMSE} = \frac{\sum_i [y_{\mathrm{model}}(n_i) - y_{\mathrm{data}}(n_i)]^2}{\sum_i [y_{\mathrm{data}}(n_i)]^2}, \quad (4)$$

where y_{model} is the model response obtained by substituting the computed kernels into Eq. (1) and y_{data} is the sequence of amplitudes of the population spikes recorded at CA1. Small NMSE values indicate that the kernels reliably capture the nonlinear dynamics of the system they model. Larger NMSE values suggest that higher order terms are needed or that the data are noisy. The NMSE is also used to determine number of Laguerre functions (L) and the Laguerre alpha (α) parameter. Values L and α are chosen to minimize the prediction NMSE and are evaluated individually for every dataset. Details on the estimation of the kernels from impulse-input and spike-output dataset can be found in Gholmieh *et al.*[15] It should be noted that that the terms in the Volterra–Poisson Series are not orthogonal to each other.[22]

Paired impulse facilitation function

The traditional descriptor of STP has been the Paired Impulse Facilitation Function (PIFF), defined as the ratio of the conditioned response amplitude over the unconditioned response amplitude to a pair of impulse stimuli with a specific interimpulse interval.[8,19] Mathematically, the PIFF can be expressed as:

$$\mathrm{PIFF}(\Delta n) = \frac{Y_2}{Y_1}, \quad (5)$$

where Y_1 is the amplitude of the population spike response to the first impulse (unconditioned response), Y_2 is the amplitude of the population spike response to the second impulse (conditioned response), Δn is the

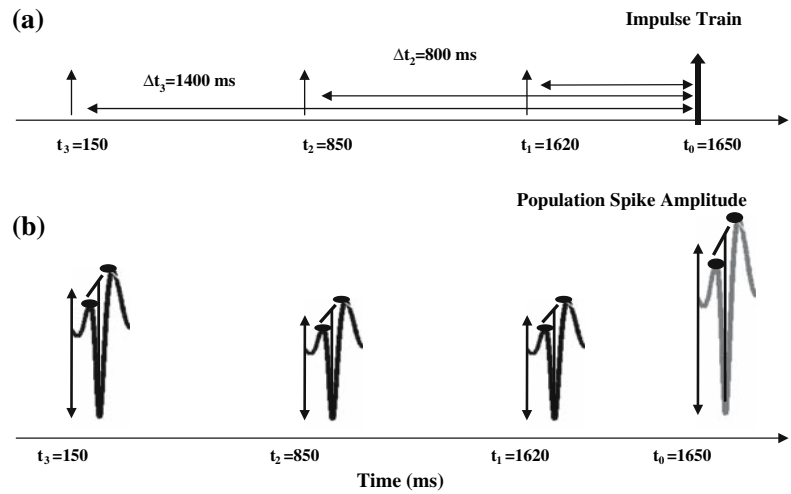

FIGURE 2. Predictive Power of Kernels. (a) A series of input electrical stimuli applied through a stimulating electrode to the Schaffer Collaterals. (b) The corresponding population spikes recorded. The amplitude of population spike was measured as the distance between the population spike minimum and the projection of the minimum on the line that joins the two positive peaks. The amplitude of the response for the last impulse (bold arrow, at 1650 ms) can be estimated using the first order kernel, the second order kernel, the third order kernel and Eq. (1). That is:

$$\begin{aligned} \boldsymbol{y}(\mathbf{1650}) = \; & \boldsymbol{k}_1 + \boldsymbol{k}_2(\Delta \boldsymbol{t}_1) + \boldsymbol{k}_2(\Delta \boldsymbol{t}_2) + \boldsymbol{k}_2(\Delta \boldsymbol{t}_3) \\ & + \boldsymbol{k}_3(\Delta \boldsymbol{t}_1, \Delta \boldsymbol{t}_1) + \boldsymbol{k}_3(\Delta \boldsymbol{t}_1, \Delta \boldsymbol{t}_2) + \boldsymbol{k}_3(\Delta \boldsymbol{t}_1, \Delta \boldsymbol{t}_3) \\ & + \boldsymbol{k}_3(\Delta \boldsymbol{t}_2, \Delta \boldsymbol{t}_1) + \boldsymbol{k}_3(\Delta \boldsymbol{t}_2, \Delta \boldsymbol{t}_2) + \boldsymbol{k}_3(\Delta \boldsymbol{t}_2, \Delta \boldsymbol{t}_3) \\ & + \boldsymbol{k}_3(\Delta \boldsymbol{t}_3, \Delta \boldsymbol{t}_1) + \boldsymbol{k}_3(\Delta \boldsymbol{t}_3, \Delta \boldsymbol{t}_2) + \boldsymbol{k}_3(\Delta \boldsymbol{t}_3, \Delta \boldsymbol{t}_3) \\ & = \boldsymbol{k}_1 + \boldsymbol{k}_2(\Delta \boldsymbol{t}_1) + \boldsymbol{k}_2(\Delta \boldsymbol{t}_2) + \boldsymbol{k}_2(\Delta \boldsymbol{t}_3) \\ & + \boldsymbol{k}_3(\Delta \boldsymbol{t}_1, \Delta \boldsymbol{t}_1) + \boldsymbol{k}_3(\Delta \boldsymbol{t}_2, \Delta \boldsymbol{t}_2) + \boldsymbol{k}_3(\Delta \boldsymbol{t}_3, \Delta \boldsymbol{t}_3) \\ & + \mathbf{2} * \boldsymbol{k}_3(\Delta \boldsymbol{t}_1, \Delta \boldsymbol{t}_2) + \mathbf{2} * \boldsymbol{k}_3(\Delta \boldsymbol{t}_1, \Delta \boldsymbol{t}_3) + \mathbf{2} * \boldsymbol{k}_3(\Delta \boldsymbol{t}_2, \Delta \boldsymbol{t}_3). \end{aligned}$$

interimpulse interval (i.e., $\Delta n = n_2 - n_1$ where n_1 is the time of occurrence of the first impulse and n_2 is the time of occurrence of the second impulse). PIFF values greater than one indicate facilitation while PIFF values less than one are interpreted as depression.

Using the PIFF defined in Eq. (2) as the STP descriptor, we can express the conditioned response $Y(\Delta n)$ in terms of the unconditioned response Y_1 and the interimpulse interval Δn as follows:

$$Y(\Delta n) = Y_1 \mathrm{PIFF}(\Delta n). \tag{6}$$

Using the Volterra–Poisson model of Eq. (1), we can express an estimate of the conditioned response as follows:

$$\overline{\overline{Y}}(\Delta n) = k_1\left(1 + \frac{k_2(\Delta n)}{k_1} + \frac{k_3(\Delta n, \Delta n)}{k_1}\right), \tag{7}$$

where the term $\left(1 + \frac{k_2(\Delta n)}{k_1} + \frac{k_3(\Delta n, \Delta n)}{k_1}\right)$ is an estimate of the PIFF.

Impulse train function (ITF)

A more recent STP descriptor has been the Impulse Train Function (ITF), defined as the ratio of the conditioned response evoked by each impulse of an impulse train stimulus over the unconditioned response evoked by the first impulse of the impulse train stimulus. Mathematically, the ITF can be expressed as:

$$\mathrm{ITF}(\Delta n_i) = \frac{Y_i}{Y_1}, \tag{8}$$

where Y_1 is the amplitude of the population spike response to the first impulse, Y_i is the amplitude of the population spike response to the i-th impulse, Δn_i is the interimpulse interval between the first impulse and the i-th impulse (i.e., $\Delta n_i = n_i - n_1$ where n_1 is the time of occurrence of the first impulse and n_i is the time of occurrence of the i-th impulse [$i > 1$]). ITF values greater than one indicate facilitation while ITF values less than one are interpreted as depression.

Using the ITF defined in Eq. (8) as the STP descriptor, we can express the amplitude of the population spike response to the i-th impulse (Y_i) in terms of the unconditioned response Y_1 and the interimpulse interval Δn_i as follows:

$$Y_i = Y_1 \mathrm{ITF}(\Delta n_i). \tag{9}$$

Considering the computed STP kernels and Eq. (1), we can derive an estimate of the conditioned responses (Y_i), expressed mathematically as:

$$\overline{\overline{Y}}_i = k_1 \left(1 + \frac{1}{k_1} \sum_i k_2(\Delta n_i) + \frac{1}{k_1} \sum_{\substack{1<j<i \\ 1<k<i}} k_3(\Delta n_j, \Delta n_k) \right), \tag{10}$$

where the term $\left(1 + \frac{1}{k_1} \sum_i k_2(\Delta n_i) + \frac{1}{k_1} \sum_{\substack{1<j<i \\ 1<k<i}} k_3(\Delta n_j, \Delta n_k) \right)$ is an estimate of the ITF.

Finally, the PIFF, estimated based on two impulse model, can still be used to predict the amplitude in fixed frequency impulse trains using the following equation:

$$Y_i = Y_{i-1}\mathrm{PIFF}(\Delta n), \tag{11}$$

where Y_i is the predicted amplitude of the population spike to the i-th impulse, Y_{i-1} is the amplitude of the population spike to the i-th − 1 impulse, and Δn is the fixed interimpulse interval.

RESULTS

The kernel STP descriptors (k_1, k_2, k_3) of the CA1 hippocampal region were computed using experimental data from *in vitro* preparations of hippocampal slices. We used fixed amplitude Poisson distributed RIT stimuli (2 Hz average rate). We applied the stimuli at the Schaffer collaterals and we recorded the resulting population spikes at the CA1 cell body layer.

CA1 STP Characteristics

Six experiments were conducted using random impulse train stimulation in the CA1 hippocampus *in vitro*. The stimulus level was chosen to correspond to values below 15% of the maximum recorded response (947 ± 73 μV) reported in the I/O curve. The data were analyzed using the adapted Volterra–Poisson method outlined in the Materials and Methods section. The number of Laguerre functions (L = 9 for all six datasets) and alpha (α = 0.93 for five datasets and 0.94 for one dataset) were determined using the prediction NMSE.[15] The first, second, and third order STP descriptors were computed. The mean population spike (k_1) was 257.43 μV (SD 31.45 μV). Comparing k_1 to the average response value reported by the I/O curve (147.77 ± 24.21 μV), we see that the 2 Hz RIT stimuli caused approximately a 70% increase in the baseline (from 147.77 to 255.69 μV).

The computed second order STP descriptors (k_2) were characterized by a fast rising facilitatory phase [0–25 ms], a peak between 25 and 50 ms, a fast declining facilitatory phase [50–200 ms], and a slow inhibitory relaxation phase [200–2000 ms]. The extent (memory) of k_2 was in the range of 1600–2000 ms. The peak of k_2 was 252% (SD 10.1%) of the value of the corresponding k_1 and occurred at 27 ms (SD 1.82 ms). Figure 3 shows the averaged second order kernel (k_2) function across six experiments in black delimited by one standard deviation in gray.

The computed third order STP descriptors (k_3) were characterized by an inhibitory area in the range of (5–100 ms, 5–100 ms), a peak inhibition at the (35 ms, 35 ms), and a mild facilitatory area in the range of (5–50 ms, 100–200 ms) and (100–200 ms, 5–50 ms). The inhibitory peak of k_3 was –75.1% (SD 11.2%) of the value of the corresponding k_1. The extent (memory) of k_3 was in the range of 250 ms. Figure 4b shows the averaged third order kernel while Fig. 4b show the variation of the third order kernel values at one standard deviation.

A Mathematical Model for STP

The computed STP kernel estimates in conjunction with Eq. (1) define a mathematical model of STP: the third order Volterra–Poisson STP model. The representation of STP by the Volterra–Poisson model provides a tool to predict population spike response amplitudes to arbitrary input patterns of impulse trains.

The prediction of the output provides a quantitative measure to evaluate the quality of the kernels and the accuracy of the model. In particular, we used the prediction error in the form of the Normalized Mean Square Error (NMSE), defined as the ratio of the sum-of-squares of the output residuals over the

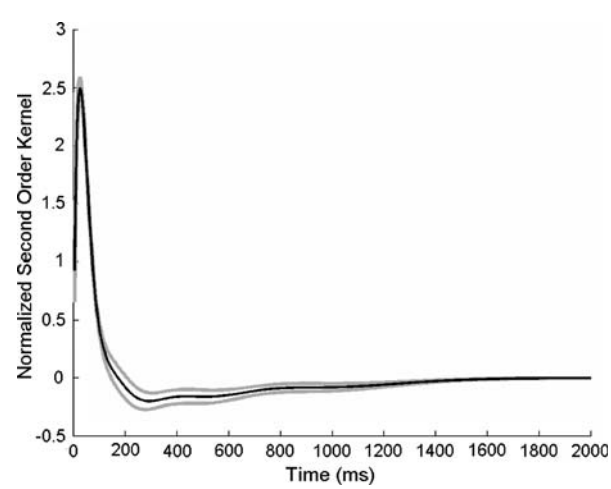

FIGURE 3. Second order kernel (black curve) delimited by one standard deviation (gray curves).

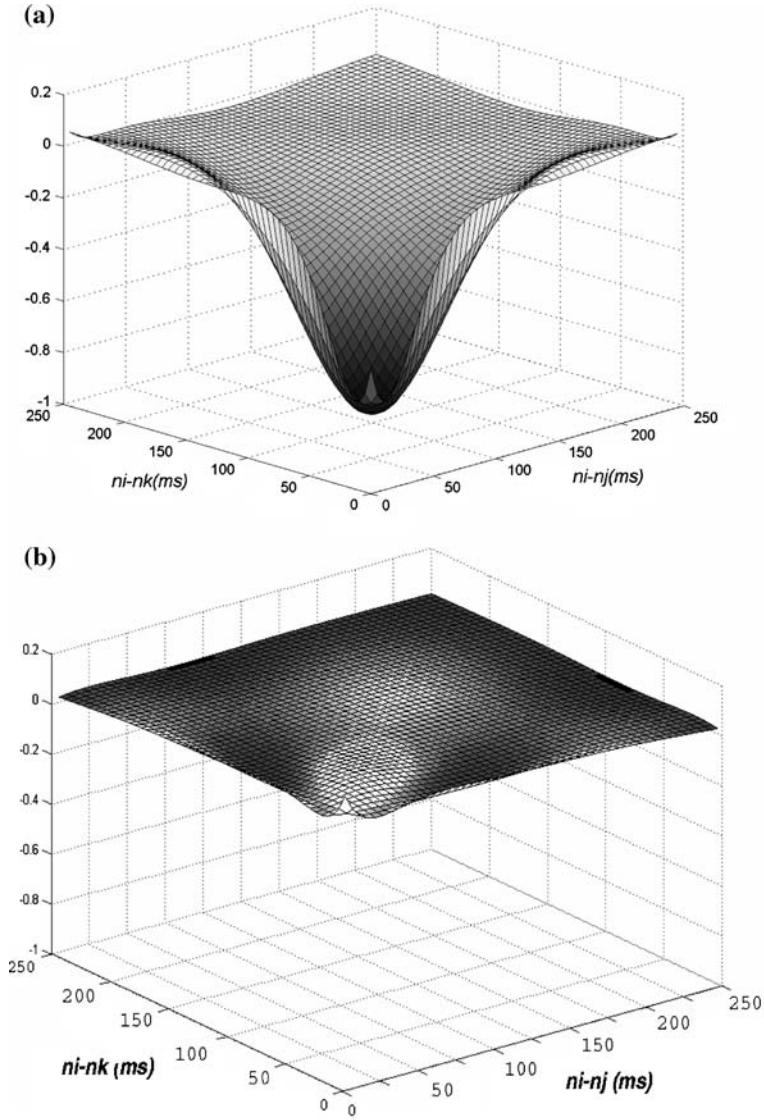

FIGURE 4. Third order kernel. (a) Third Order kernel calculated using the averaged Laguerre coefficient values. (b) Third order kernel standard deviation.

sum-of-squares of the recorded response amplitudes to evaluate the accuracy of the kernels and the STP model. Small NMSE values indicate that the STP descriptors sufficiently captured the underlying nonlinear STP dynamics and that the associated STP model is reliable. Large NMSE values suggest that higher order terms (fourth, fifth etc.) need to be included or that the data were noisy. The third order Volterra–Poisson STP model for the CA1 case exhibited an average in-sample prediction NMSE of 19.7% (SD 4.90%) when the first and second order terms were used, and 5.3% (SD 0.5%) when the first, second, and third order terms were included in the model. The third order term improved the in-sample prediction accuracy of the model by 14.4%.

One of the biggest strengths of the proposed Volterra–Poisson model of STP is that it provides response prediction to arbitrary impulse sequence stimuli. We demonstrate this by employing the in-sample and the out-of-sample prediction paradigm that involves the following steps: (1) STP kernels were computed using data from all the recorded datasets; (2) the stimulus from all the datasets was used as the input/output to estimate the third order model, and the resulting model response to a specific subset (in-sample prediction) was compared to the corresponding recorded response; (3) recordings excluding a specific subset were used again as the input/output to estimate the third order model, and the resulting model response to the excluded stimuli (out-of-sample prediction) was compared to the corresponding recorded response. Figure 5a shows a segment of in-sample model response (circles) and the corresponding data points of the recorded response

(diamonds). Figure 5b shows a segment of out-of-sample predicted response (squares) and the corresponding data points of the recorded response (diamonds). In the case shown in Fig. 5, comparison of the out-of-sample predicted response to the corresponding in-sample predicted response showed that NMSE values were very close, i.e., 18.72% (in-sample) vs. 22.32% (out-of-sample) using the first and second order terms and 5.96% (in-sample) vs. 8.14% (out-of-sample) using the first, second, and third order terms. In general, the third order model average in-sample prediction NMSE was 5.25% (SD 0.6%) and the average out-of-sample prediction NMSE was 7.24% (SD 1.8%). The low NMSE values validated the accuracy of the third order model and confirmed the importance of the third order term.

Kernel STP Descriptors and the Paired Impulse Facilitation Function (PIFF)

The computed STP prediction model was tested for the ability to predict paired impulse generated data. Six experiments were conducted using paired impulse stimuli with impulse intervals in the range of [10–600 ms] with the same experimental setup and aCSF solution as in the case of random impulse train stimuli. We compared the predictive capability of the PIFF and the third order Volterra–Poisson model. First, we used the Volterra–Poisson STP model to predict the conditioned response amplitude out of an impulse pair at various interimpulse intervals. Figure 6a shows the average experimental values of the conditioned response amplitude (black line), the predicted conditioned response amplitude values using the first two terms (first and second order term) of the Volterra–Poisson model (light gray line), and the predicted conditioned response amplitude using all three terms of the model (dark gray line) over a range of interimpulse intervals [10–600 ms]. The resulting NMSE was 16.5% when the first two terms were used and 4.83% when all three terms were included. Clearly, the Volterra Poisson STP model could predict accurately the conditioned response amplitude, especially when the third order term was included. Next, we used the PIFF to predict population spike response amplitudes from the RIT stimulus experiment and compared it to the corresponding predicted response using the third order Volterra–Poisson STP model. The NMSE was 7.29% when the PIFF (Eq. 3) was used and 2.56% when the Volterra–Poisson STP model was used (Eq. 1). Figure 6b shows the recorded amplitude responses (diamonds), the predicted responses using PIFF (squares), and the Volterra–Poisson STP model prediction (gray circles). A comparison between predicted responses using the PIFF and predicted responses using the Volterra–Poisson STP model suggests that the third order Volterra–Poisson STP model can predict population spike response amplitudes evoked by RIT stimuli better than PIFF. This may be attributed to the fact that neither the estimation of PIFF nor the PIFF

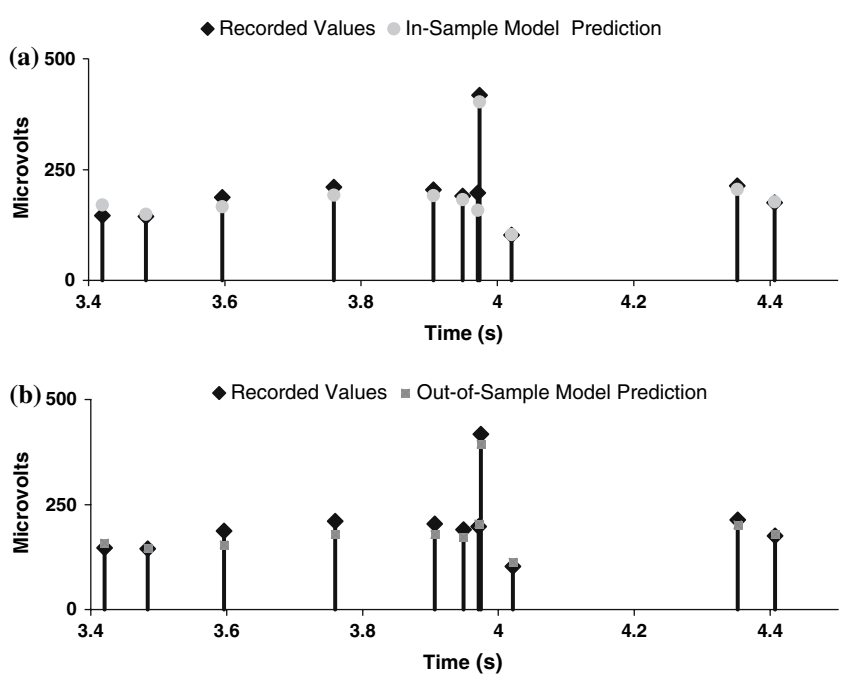

FIGURE 5. Predictive Power of kernels. (a) Segment of recorded responses (black diamonds) and In-Sample predicted responses (light gray circles). (b) Segment of recorded responses (black diamonds) and Out-of-Sample predicted responses (dark gray squares).

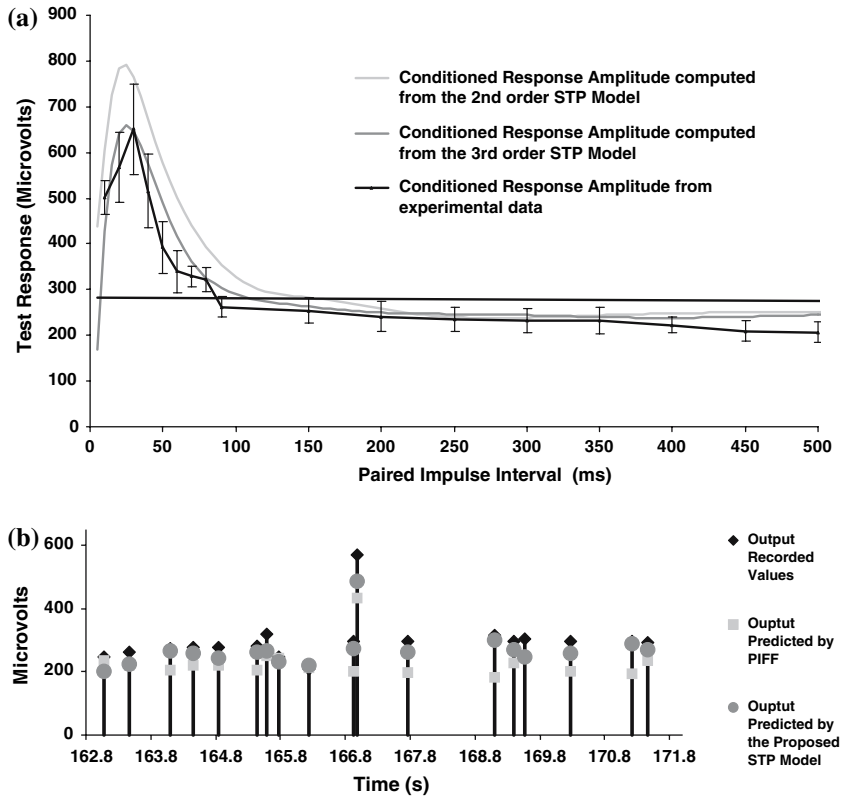

FIGURE 6. (a) A plot of recorded conditioned responses (black) predicted using the Volterra–Poisson STP model (predicted conditioned responses using the first and second order kernels are shown in light gray; predicted conditioned responses using the first, second, and third order kernels are shown in dark gray). (b) Sample of the recorded population spike amplitude responses to RIT stimuli (diamonds), the predicted responses using PIFF (squares), and the Volterra–Poisson STP model (circles). A comparison between predicted responses using the PIFF and predicted responses using the Volterra–Poisson STP model suggests that the third order Volterra–Poisson STP model can better predict the population spike response amplitudes evoked by the RIT stimuli.

based prediction took into account interactions between the current impulse stimulus and impulse stimuli beyond the previous one.

Kernel STP Descriptors and the Impulse Train Function (ITF)

The developed third order Volterra–Poisson STP model was used to predict fixed frequency train data (Eq. 8). Four experiments were conducted using impulse train stimuli at the following interimpulse intervals: 40, 80, 100, 150, and 200 ms. The corresponding population spike amplitude responses up to the 4th impulse are shown in Fig. 7a–e for the 40, 80, 100, 150, and 200 ms interimpulse intervals, respectively (black diamonds). The corresponding predicted values using the presented Volterra-Poisson STP model are also shown in Fig. 7. The light gray line with black crosses denotes predicted amplitude responses using the PIFF. The light gray triangles denote predicted amplitude responses when only the first two terms of the model were used and the dark gray squares denote the predicted amplitude responses when all the three terms of the Volterra–Poisson model were used. The average prediction NMSE was 65.3% for the 40 ms, 77.4% for the 80 ms, 163.3% for the 100 ms, 94.7% for the 150 ms, and 17.9% for the 200 ms interimpulse interval when the PIFF was used. The average prediction NMSE was 151.1% for the 40 ms, 16.4% for the 80 ms, 7.23% for the 100 ms, 11.68% for the 150 ms, and 11.81% for the 200 ms interimpulse interval when the first two terms were used. The average prediction NMSE using all the terms of the model was 17.3% for the 40 ms, 1.36% for the 80 ms, 1.47% for the 100 ms, 10.55% for the 150 ms, and 11.14% for the 200 ms interimpulse intervals. It can be readily concluded that the third order STP model was able to predict the values of the impulse trains with higher accuracy.

It should also be noted that in the case of the 40 ms impulse train, the inclusion of the third order term brought the NMSE down from 151 to 17.3% in the case where the first and the second order terms were used, an impressive 133%. This can be explained by the significant inhibition behavior of the third order kernel

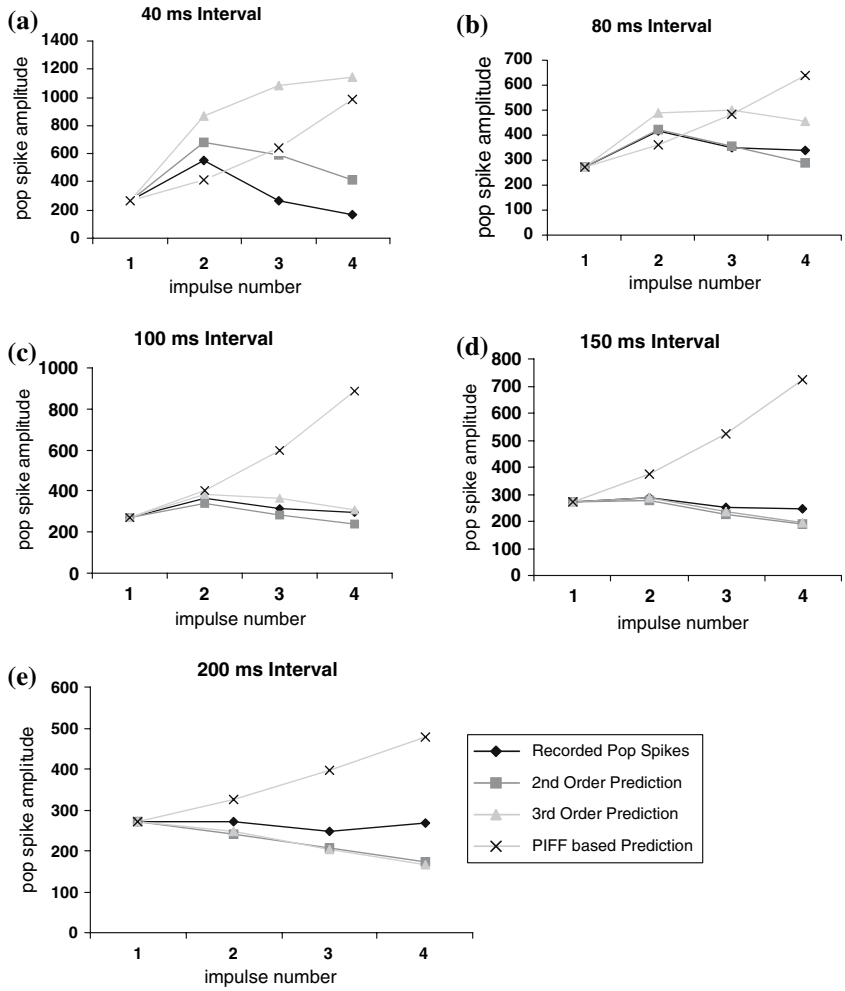

FIGURE 7. Representative impulse sequences at the following intervals: (a) 40 ms, (b) 80 ms, (c) 100 ms, (d) 150 ms, (e) 200 ms. Recorded population spike amplitudes are represented as black diamonds. ITF values predicted using the PIFF are shown in black crosses; ITF values predicted using the first two terms of the third order model are shown in light gray triangles; ITF values predicted using the third order model are shown in dark gray squares.

in the range of (5–50 ms, 5–50 ms) with a negative peak around (35 ms, 35 ms) [Fig. 4a]. In contrast to the third order model, the PIFF failed significantly in predicting the responses amplitude at 100 and 150 ms intervals since it does not take into consideration the inhibitory component inherent in the stimulation history.

DISCUSSION

Traditionally, CA1 short-term plasticity has been investigated using paired impulse stimuli with fixed amplitude and variable interimpulse interval and impulse trains of fixed amplitude and frequency, varying the frequency from one experimental run to another. In each case, the behavior of the STP mechanisms has been captured by description functions defined arbitrarily by each method, i.e., the Paired Impulse Facilitation Function (PIFF) and the impulse train function (ITF). A more realistic paradigm for characterizing STP is the application of point-process stimuli such as impulse train stimuli with randomly varying interimpulse interval[2,30,32,34] and natural stimuli patterns.[10] Point-process stimuli trigger nonlinear dynamic behaviors that are more complex than those evoked by pairs or short trains of impulses. This type of nonlinear dynamic complexity requires the scalable and mathematically rigorous modeling approach provided by the Volterra–Poisson method. The computed Volterra–Poisson kernels captured quantitatively the dynamic nonlinearties of the CA1 STP with high degree of accuracy as supported by the small predictive error of the proposed third order Volterra–Poisson STP model.

The computed second order STP descriptor (k_2) was characterized by a fast rising facilitatory phase

[0–25 ms], a peak between 25 and 50 ms, a fast declining facilitatory phase [50–200 ms], and a slow inhibitory relaxation phase [200–2000 ms]. The memory of the second order dynamics (reflected by the extent of k_2) in the CA1 system *in vitro* was found to be at most 2 s. The temporal extent of k_2 is in agreement with a study conducted by Fuhrman *et al.*[13] showing that depressing and excitatory synapses are modulated by 4–8 presynaptic spikes. The third order kernel had an inhibitory area (0–100,0–100) ms indicating that in a high frequency train (10–50 Hz), the second response is always larger then the third one, a property that may have a physiological significance.[5]

The third order Volterra–Poisson STP model was able to predict in-sample and out-of-sample RIT data accurately. A comparison between the third order Volterra–Poisson model and the commonly used PIFF and ITF functions was undertaken to further test the predictive power of the proposed model. The PIFF did not predict random impulse train responses as accurately while the calculated kernels were able to approximate the PIFF characteristics. The third order model was able to track the STP dynamics of short trains. ITF, on the other hand, could not be used in a meaningful way to predict random interval train data. Hence, the resulting kernel expansion provided a good prediction framework of impulse trains drawn from the stimulus ensemble of Poisson distributed impulse trains. The third order model also provided a good description of the responses to other classic impulse trains (paired impulse and fixed frequency impulse trains). In general, if a third-order model does not provide adequate prediction power for other classes of stimuli, the order of the estimated kernels can be tuned by testing higher order models.

In contrast to the traditional PIFF studies[8,19,26] our results suggest that long intervals induce inhibition under continuous stimulation leading to a balance between excitation and inhibition. These results parallel findings by Fuhrman *et al.*[13] indicating that depressing and excitatory synapses are optimized in the 0.5–5 Hz and 9–70 Hz frequency range, respectively.

This frequency optimization might play a role in Long-Term Potentiation (LTP) and Depression (LTD). LTP and LTD are two processes that are thought to play a major role in memory formation through Hebbian learning. LTP is usually elicited *in vitro* using high frequency trains (50–200 Hz) that correspond to the facilitation range of the second order kernel. LTD, on the other hand is usually elicited *in vitro* using low frequency trains ($\sim$1 Hz) that correspond to the inhibitory region of the second order kernel. Our results suggest that an active cell (constantly bombarded by action potentials) is optimized for the induction process of LTP and LTD, an observation not readily seen using PIFF.

In a recent study, using natural pattern of stimulation,[10] it was concluded that the response amplitude is not a function of the preceding interimpulse interval. We would argue that the results obtained did not show any temporal relationship because the analysis of the burst activities found in the natural pattern did not include a model that could capture complex spike interactions such as the one used in this paper.

The work presented in this paper lays the foundation for understanding at the electrophysiological level how the hippocampus creates associations dynamically between different sensory modalities in order to learn and remember spatial relations among multiple, complex environmental cues. Although, it studies the single-input/single-output case, the proposed model can be extended to include multi-inputs and multi–outputs with the potential to offer a deeper understanding of how different pathways interact in the hippocampus (e.g., the medial and lateral pathways in the Dentate Gyrus, and the commissural fibers with the Schaffer collaterals in the CA1 region) and the brain in general.

ACKNOWLEDGMENTS

This work was supported by Grant No. RR-01861 from the Division of Research Resources of the National Institutes of Health and by Grants 0646 and 0259 from DARPA Controlled Biological Systems Program and the Office of Naval Research.

REFERENCES

[1]Abbott, L. F., J. A. Varela, K. Sen, and S. B. Nelson. Synaptic depression and cortical gain control. *Science* 275:220–224, 1997.

[2]Berger, T. W., J. L. Eriksson, D. A. Ciarolla, and R. J Sclabassi. Nonlinear systems analysis of the hippocampal Perforant Path-Dentate projection. II Effects of random train stimulation. *J. Neurophysiol.* 60:1077–1094, 1988.

[3]Berger, T. W., J. L. Eriksson, D. A. Ciarolla, and R. J. Sclabassi. Nonlinear systems analysis of the hippocampal Perforant Path-Dentate projection. III Comparison of random train and paired impulse stimulation. *J. Neurophysiol.* 60:1095–1109, 1988.

[4]Buonomano, D. V. Distinct functional types of associative Long-Term Potentiation in the neocortical and hippocampal pyramidal neurons. *J. Neurosci.* 19(16):6748–6754, 1999.

[5]Buonomano, D. V. Decoding temporal information: A model based on short-term synaptic plasticity. *J. Neurosci.* 20(3):1129–1141, 2000.

[6]Castellucci, V. F. and E. R. Kandel. A quantal analysis of the synaptic depression underlying habituation of the gill-withdrawal reflex in Aplysia. *Proc. Natl. Acad. Sci. USA* 71(12):5004–5008, 1974.

[7]Castro-Alamancos, M. A. and B. W. Connors. Distinct forms of short-term plasticity at excitatory synapses of

hippocampus and neocortex. *Proc. Natl. Acad. Sci. USA* 94:4161–4166, 1997.

[8]Creager, R., T. Dunwiddie, and G. Lynch. Paired-pulse and frequency facilitation in the CA1 region of the *in vitro* rat hippocampus. *J. Neurophysiol.* 299:409–424, 1980.

[9]Courellis, S. H., V. Z. Marmarelis, and T. W. Berger. Modeling event-driven nonlinear dynamics in neuronal systems with multiple inputs. Annual Conference Biomedical Engineering Society, Seattle, WA, 2000.

[10]Dobrunz, L. E. and C. F. Stevens. Response of hippocampal synapses to natural stimulation patterns. *Neuron* 22(1):157–166, 1999.

[11]Ferster, D. and N. Spruston. Cracking the neuronal code. *Science* 270:756–757, 1995.

[12]Fortune, E. S. and G. R. Rose. Short-term synaptic plasticity contributes to the temporal filtering of electrosensory information. *J. Neurosci.* 20(18):7122–7130, 2000.

[13]Fuhrmann, G., I. Segev, H. Markram, and M. Tsodyks. Coding of temporal information by activity-dependent synapses. *J. Neurophys.* 87:140–148, 2002.

[14]Gerstner, W., A. Kreiter, H. Markram, and A. Herz. Neural codes: Firing rate and beyond. *Proc. Natl. Acad. Sci. USA* 94:12740–12741, 1997.

[15]Gholmieh, G., S. H. Courellis, V. Z. Marmarelis, and T. W. Berger. An efficient method for modelling short term plasticity using random impulse stimuli. *J. Neurosci. Methods* 21(2):111–127, 2002.

[16]Gholmieh, G., S. H. Courellis, V. Z. Marmarelis, T. W. Berger, and M. Baudry. A biosensor for detecting changes in cognitive processing based on nonlinear systems analysis. *Bios. Bioelec.* 16(7–8):491–501, 2001.

[17]Gross, G. W., B. K. Rhoadas, D. L. Reust, and F. U. Schwalm. Stimulation of monolayer networks in culture through thin film indium-tin oxide recording electrodes. *J. Neurosci. Methods* 50:131–143, 1993.

[18]Konig, P., A. K. Engel, and W. Singer. Integrator or coincidence detector? the role of the cortical neuron revisited. *Trends Neurosci* 19:130–137, 1996.

[19]Leung, L. S. and X. W. Fu. Factors affecting paired-pulse facilitation in the hippocampal CA1 neurons in vitro. *Brain Res.* 650:75–84, 1994.

[20]Markram, H. and M. Tsodyks. Redistribution of synaptic efficacy between neocortical pyramidal neurons. *Nature* 382:807–810, 1996.

[21]Marmarelis, V. Z. Nonlinear Dynamic Modeling of Physiological Systems. Wiley, New York, NY, 2004.

[22]Marmarelis, V. Z. and T. W. Berger. General methodology for nonlinear modeling of neural systems with Poisson point-process inputs. *Math. Biosci.* 196:1–13, 2005.

[23]Michelson, H. B., J. Kapur, and E. W. Lothman. Reduction of paired pulse inhibition in the CA1 region of the hippocampus by pilocarpine in naive and in amygdala-kindled rats. *Exp. Neurol.* 104(3):264–271, 1989.

[24]O'Donovan, M. J. and J. Rinzel. Synaptic depression: A dynamic regulator of synaptic communication with varied functional roles. *Trends Neurosci.* 20:431–432, 1997.

[25]Pananceau, M, H. Chen, and B. Gustafsson. Short-term facilitation evoked during brief afferent tetani is not altered by long-term potentiation in the guinea-pig hippocampal CA1 region. *J. Physiol.* 508(2):503–514, 1998.

[26]Papatheodoropoulos, C. and G. Kostopoulos. Dorsal-ventral differentiation of short-term synaptic plasticity in rat CA1 hippocampal region. *Neurosci. Lett.* 286(1):57–60, 2000.

[27]Richmond, B. J. and L. M. Optican. Temporal encoding of two-dimensional patterns by single units in primate visual cortex. II. Information transmission. *J. Neurophysiol.* 64:370–380, 1990.

[28]Rieke, F., D. Waarland, R. R. De Ruyter Van Steveninck, and W. Bialek. Spikes: Exploring the Neural Code. MIT Press, Cambridge, MA, 1997.

[29]Senn, W., I. Segev, and M. Tsodyks. Reading neuronal synchrony with depressing synapses. *Neural Comput.* 10:815–819, 1998.

[30]Sclabassi, R. J., J. L. Eriksson, R. Port, G. Robinson, and T. W. Berger. Nonlinear systems analysis of the hippocampal Perforant Path-Dentate Projection I. Theoretical and interpretational considerations. *J. Neurophysiol.* 60:1066–1076, 1988.

[31]Stringer, J. L. and E. W. Lothman. In vitro effects of extracellular calcium concentrations on hippocampal pyramidal cell responses. *Exp. Neurol.* 101(1):132–146, 1988.

[32]Tsodyks, M. V. and H. Markram. The neural code between neocortical pyramidal neurons depends on neurotransmitter release probability. *Proc. Natl. Acad. Sci. USA* 94:719–723, 1997.

[33]Valentin, A., J. J. Garcia-Seoane, and A. Colino. Lithium enhances synaptic transmission in neonatal rat hippocampus. *Neuroscience* 78(2):385–391, 1997.

[34]Varela, J. A., K. Sen., J. Gibson, J. Fost, L. F. Abbot, and S. B. Nelson. A quantitative description of short-term plasticity at excitatory synapses in layer 2/3 of the visual cortex. *J. Neurosci.* 17:7926–7940, 1997.

[35]Westwick, D. T., B. Suki, and K. R. Lutchen. Sensitivity analysisof kernel estimates: Implications in nonlinear physiological systemidentification. *Ann. Biomed. Eng.* 26(3):488–501, 1998.

[36]Zucker, R. S Short-term synaptic plasticity. *Ann. Rev. Neurosci.* 12:13–31, 1998.